# Controller Hardware-in-the-Loop Evaluation of a Microgrid Controller for a Microgrid System with Multiple Grid-Forming Inverters

## Preprint

Fuhong Xie,[1] Shashank Singh,[2] Jing Wang,[1] Subhankar Ganguly,[1] Wenzong Wang,[3] Rahul R. Jha,[4] and Jacqueline Baum[3]

*1 National Renewable Energy Laboratory*
*2 Siemens Technology and Services Private Limited*
*3 Electric Power Research Institute*
*4 Commonwealth Edison*

*To be presented at the 2024 IEEE Energy Conversion Conference and Expo*
*Phoenix, Arizona*
*October 20–24, 2024*

**NREL is a national laboratory of the U.S. Department of Energy**
**Office of Energy Efficiency & Renewable Energy**
**Operated by the Alliance for Sustainable Energy, LLC**

This report is available at no cost from the National Renewable Energy Laboratory (NREL) at www.nrel.gov/publications.

Contract No. DE-AC36-08GO28308

**Conference Paper**
NREL/CP-5D00-89074
September 2024

# Controller Hardware-in-the-Loop Evaluation of a Microgrid Controller for a Microgrid System with Multiple Grid-Forming Inverters

## Preprint

Fuhong Xie,[1] Shashank Singh,[2] Jing Wang,[1] Subhankar Ganguly,[1] Wenzong Wang,[3] Rahul R. Jha,[4] and Jacqueline Baum[3]

*1 National Renewable Energy Laboratory*
*2 Siemens Technology and Services Private Limited*
*3 Electric Power Research Institute*
*4 Commonwealth Edison*

**Suggested Citation**
Xie, Fuhong, Shashank Singh, Jing Wang, Subhankar Ganguly, Wenzong Wang, Rahul R. Jha, and Jacqueline Baum. 2024. *Controller Hardware-in-the-Loop Evaluation of a Microgrid Controller for a Microgrid System with Multiple Grid-Forming Inverters: Preprint*. Golden, CO: National Renewable Energy Laboratory. NREL/CP-5D00-89074. https://www.nrel.gov/docs/fy24osti/89074.pdf.



**NREL is a national laboratory of the U.S. Department of Energy**
**Office of Energy Efficiency & Renewable Energy**
**Operated by the Alliance for Sustainable Energy, LLC**

This report is available at no cost from the National Renewable Energy Laboratory (NREL) at www.nrel.gov/publications.

Contract No. DE-AC36-08GO28308

**Conference Paper**
NREL/CP-5D00-89074
September 2024

National Renewable Energy Laboratory
15013 Denver West Parkway
Golden, CO 80401
303-275-3000 • www.nrel.gov

## NOTICE

This work was authored in part by the National Renewable Energy Laboratory, operated by Alliance for Sustainable Energy, LLC, for the U.S. Department of Energy (DOE) under Contract No. DE-AC36-08GO28308. Funding provided by U.S. Department of Energy Office of Energy Efficiency and Renewable Energy Solar Energy Technologies Office under Award Number DE-EE0009336. The views expressed herein do not necessarily represent the views of the DOE or the U.S. Government.

# Controller Hardware-in-the-Loop Evaluation of a Microgrid Controller for a Microgrid System with Multiple Grid-Forming Inverters

Fuhong Xie, Jing Wang, Subhankar Ganguly
*Power Systems Engineering Center*
*National Renewable Energy Laboratory*
Golden, CO USA
Fuhong.Xie, Jing.Wang, Subhankar.Ganguly@nrel.gov

Shashank Singh
*Grid Software*
*Siemens Technology and Services Private Limited*
Bangalore, India
shashanksingh@siemens.com

Wenzong Wang, Jacqueline Baum
*Distributed Energy Resources Integration*
*EPRI*
Knoxville, USA
WWang, JBaum@epri.com

Rahul R Jha
*Smart Grid - Emerging technology*
*Commonwealth Edison*
Chicago, USA
Rahul.Jha@ComEd.com

***Abstract*—This paper presents the laboratory evaluation of a commercial Microgrid Management System (MGMS) implemented in the real-world Bronzeville Microgrid which features a futuristic scenario with high renewable energy integration and the use of multiple Grid-Forming (GFM) inverters. The primary objective of the performance evaluation for the MGMS is to assess the MGMS's capability to dispatch GFM units, including a GFM PV unit and two GFM battery units, to maintain the system stability and ensure economic operation, thus guaranteeing the microgrid's resilience during prolonged outages and dynamic events. The laboratory controller hardware-in-the-loop provides realistic testing environment through detailed electromagnetic transient modeling of the microgrid system, hardware MGMS, and standard communication protocols (DNP3). The CHIL evaluation shows how the MGMS effectively manages the GFM inverters, highlighting its performance in maintaining stability, reliability, and survivability in a microgrid environment with a high penetration of renewable energy sources.**

***Index Terms*—Microgrid, grid-forming inverters, distribution management system, islanding operations, controller hardware-in-the-loop.**

## I. Introduction

Microgrids have been widely deployed worldwide to enhance power system resilience and reliability due to unexpected power interruptions [1], and grid-forming (GFM) inverter(s) are replacing traditional synchronous generators as the GFM source in microgrids to achieve renewable integration targets [2]. A distribution management system (DMS) plays a key role in a microgrid system to manage the control, operation, and monitoring of the whole microgrid system to achieve system stability, generation, load balance, and economical operation [3]. However, the dispatch of GFM inverters in a microgrid system have not been well-studied in the existing literature on DMS, because GFM inverters have not yet been widely used as a frequency source in microgrids [4], especially with multiple of them working together.

With increasingly GFM inverter-based resources (IBRs) replacing traditional fossil fuel-based synchronous generators as GFM sources, the existing microgrid DMS must be updated to control GFM inverters considering system control objectives and device constraints [5]. Driven by this gap and the need for pilot demonstrations, a one-of-a-kind DMS is developed based on a real-world microgrid project to showcase how DMS can optimally dispatch multiple GFM inverters, especially when one GFM inverter driven by the photovoltaics (PV) DC source, together with other grid assets. The controller hardware-in-the-loop (CHIL) evaluation of the microgrid DMS is conducted in the laboratory environment to evaluate the performance of this microgrid DMS using the actual microgrid, real-time measurement and control, and standard industry protocols, which de-risks the technology integration before field deployment.

This paper demonstrates the MGMS's capability to effectively integrate and manage the GFM PV inverter within a microgrid system. The GFM PV inverters and other grid-forming devices play a crucial role in providing dynamic support to the microgrid, and this study shows how the MGMS can autonomously coordinate power generation from all GFM units, and ensure reliable operation even during islanded conditions. The contributions of this paper can be summarized

This work was authored in part by the National Renewable Energy Laboratory, operated by Alliance for Sustainable Energy, LLC, for the U.S. Department of Energy (DOE) under Contract No. DE-AC36-08GO28308. Funding provided by U.S. Department of Energy Office of Energy Efficiency and Renewable Energy Solar Energy Technologies Office under Award Number DE-EE0009336. The views expressed in the article do not necessarily represent the views of the DOE or the U.S. Government. The U.S. Government retains and the publisher, by accepting the article for publication, acknowledges that the U.S. Government retains a nonexclusive, paid-up, irrevocable, worldwide license to publish or reproduce the published form of this work, or allow others to do so, for U.S. Government purposes.

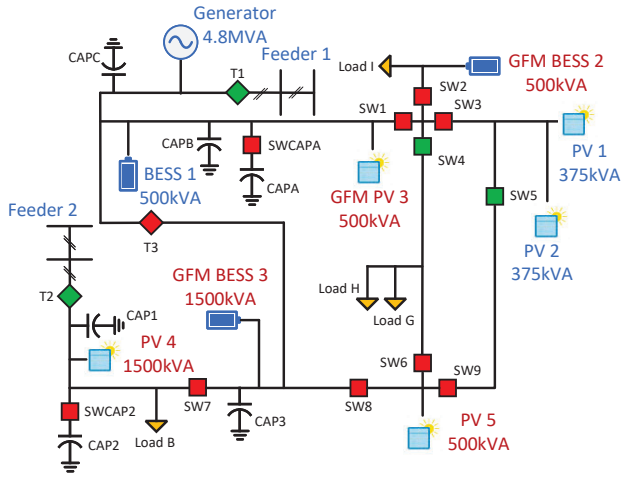


Fig. 1: The system diagram of the microgrid under testing.

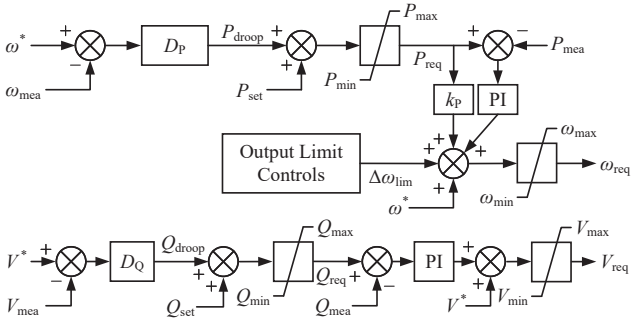


Fig. 2: Power-level control diagram for GFM inverters [6].

as follows: This paper 1) explores the parallel operation of multiple GFM inverters, including one GFM PV inverter and two GFM battery inverters; 2) deploys a commercial DMS with new functions to optimally dispatch multiple GFM inverters together with other grid assets; and 3) demonstrates the first-of-its-kind microgrid DMS through dynamic events to evaluate the stability, reliability, and survivability of the real-world microgrid system with purely IBRs.

## II. System Configurations

### A. Microgrid Settings

The Bronzeville Microgrid is the focus of this study and consists of two feeders, each with a tie-breaker at the feeder head. In islanded mode, tie-breakers T1 and T2 are open while tie-breaker T3 is closed, creating a single microgrid system. When connected to the main grid, T1 serves as the point of isolation (POI) breaker. The microgrid DMS resynchronizes to the main grid by controlling the voltage over T1.

To enhance the system, additional distributed energy resources (DERs) have been added, aiming for 75% renewable energy penetration. These additions include three PV units with capacities of 500 kVA (PV3 and PV4) and 1500 kVA (PV5), along with two battery energy storage systems (BESSs) with capacities of 500 kVA (BESS2) and 1500 kVA (BESS3). These new units, PV3, and both BESS2 and BESS3, are equipped with GFM inverters, enabling the microgrid to operate three GFM inverters in parallel. The gas generator, which is

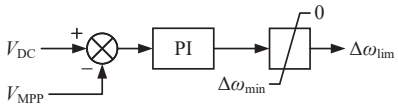


Fig. 3: Voltage limiter for GFM PV inverter.

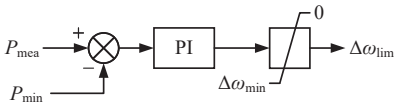


Fig. 4: Charging power limiter for GFM BESS inverter.

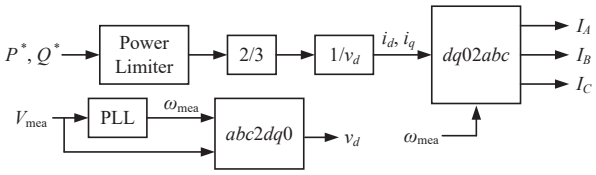


Fig. 5: Diagram of grid-following inverter modeling.

no longer the primary GFM source, remains in standby mode to provide backup if the inverter-based resources lack sufficient capacity.

### B. Grid-Forming Inverter Modeling

The control diagram of GFM inverters involves the microgrid DMS controller dispatching a frequency command ($\omega^*$), which is compared to the measured frequency ($\omega_{mea}$). The difference, multiplied by a droop gain ($D_P$), yields the necessary active power generation ($P_{droop}$) for frequency support. When an active power set point ($P_{set}$) is received, it is summed with $P_{droop}$ and compared to the actual active power ($P_{mea}$). A proportional-integral section then calculates the frequency deviation signals, while a feed-forward loop with a proportional gain ($k_P$) enhances dynamic performance.

Output limit control is incorporated into the frequency controls. For the GFM PV unit, a voltage limiter manages the DC bus voltage ($V_{DC}$), generating a negative regulation signal ($\omega_{req}$) when $V_{DC}$ is below the MPP voltage ($V_{MPPT}$). For the GFM BESS unit, an output limit controller ensures operation within power limits, generating a negative regulation signal to reduce the charging power when power falls below $P_{min}$.

Similarly, the inverter voltage command ($V^*$) is generated by the microgrid DMS controller. The error between $V^*$ and the actual local voltage ($V_{mea}$) calculates the required reactive power ($Q_{droop}$) for voltage support. After adding the reactive power set point ($Q_{set}$), the required reactive power ($Q_{req}$) is compared with the actual reactive power ($Q_{mea}$) to generate the necessary voltage signal ($V_{req}$).

### C. Grid-Following Inverter Modeling

The tested microgrid includes five grid-following (GFL) inverters modeled as controllable current sources. These inverters measure the local voltage ($V_{mea}$) and calculate the frequency angle and $d$-axis voltage ($v_d$). The microgrid DMS dispatches active ($P^*$) and reactive ($Q^*$) power commands, limited by the rated capacities of BESS and PV units and the available generation power determined by the MPPT

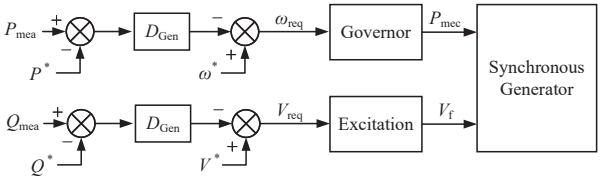


Fig. 6: Gas generator modeling.

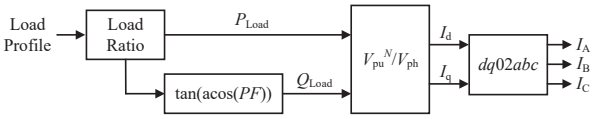


Fig. 7: Load modeling.

algorithm. The commands are divided by $v_d$ to compute the $dq$-axis currents, which are then transformed to $abc$ currents using a $dq0$-to-$abc$ transformation module. These transformed currents control three independent current sources, injecting the desired currents ($I_{ABC}$) into the grid, thus maintaining effective power flow and grid stability.

### D. Modeling of Gas Generator and Loads

The gas generator is modeled using a governor model and a standard IEEE AC1A type excitation system model. The microgrid DMS sends active and reactive power commands to the generator model, and discrepancies between the commanded and actual power are multiplied by the droop gain to adjust the generator's frequency and voltage. The generator's frequency and voltage set points are maintained at 60 Hz and 1 p.u., respectively. The governor model adjusts the mechanical power input based on the speed error to maintain the correct frequency, while the excitation system model controls the field voltage to maintain the terminal voltage.

The microgrid load module's profile is measured at the feeder's head without individual load measurements. The planning value for each load is used, and its ratio to the total load at the feeder head estimates the load value for each module. The power factor is constant at 0.9, and both phase-to-ground and per-unit phase-to-ground voltages characterize the system's voltage levels. Different load types are modeled using parameter $N$, with $N = 0$ for constant power, $N = 1$ for constant current, and $N = 2$ for constant impedance, ensuring accurate load value calculations based on overall load measurements while considering specific load characteristics.

## III. Test System Experimental Configurations

### A. Laboratory Setups of Test System

The microgrid controller utilizes a commercial DMS, the Spectrum Power Microgrid Management System (MGMS) from Siemens [8]. The DMS functions are developed based on common requirements for feeder-level microgrid controllers as specified in [9]. The configured CHIL platform is shown in Figure 8. The microgrid system is modeled in OPAL-RT using the eMEGASIM platform, with a simulation time step of 200 microseconds. Communication between the OPAL-RT (acting as the server) and the MGMS (acting as the client) is

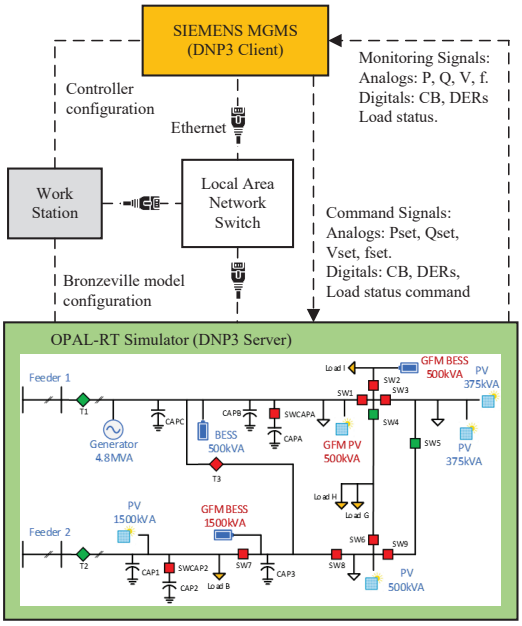


Fig. 8: Laboratory CHIL configurations.

facilitated using the Distributed Network Protocol 3 (DNP3). The setup includes a total of 26 analog set points, 147 analog measurements, 28 digital status commands, and 26 digital status indicators.

The GFM inverters are set up to operate in GFM control mode at all times, even when connected to the grid. These inverters receive voltage ($V^*$) and frequency ($\omega^*$) set points from the MGMS. The remaining GFL DERs and the generator receive active ($P^*$) and reactive ($Q^*$) power set points.

The primary objectives of testing the MGMS are to 1) evaluate the performance of the dispatch and transition functions based on the IEEE 2030.7 standard [10] and 2) assess the overall performance of the system, including the coordinated control between the MGMS and DERs, using performance metrics defined in [9].

### B. System Grid-Forming Inverter Controls and Droop Settings

The paper aims to evaluate the ability of the DMS to provide secondary frequency and voltage control during island operation. The MGMS ensures frequency and voltage restoration across the microgrid, maintaining stability at the feeder level through droop-based load sharing among multiple GFM DERs. The primary controls of GFM DERs adjust system frequency and voltage based on power output, and the MGMS shifts the droop curve to maintain these values around their rated levels.

Both the GFM BESS and GFM PV units share the same droop settings for active and reactive power, allowing for equal power sharing. The GFM BESS unit has defined maximum and minimum power levels based on its capacity, and it quickly increases system frequency when operating power reaches the minimum level by adopting a vertical $P$-$f$ droop curve, reducing the charging power. The GFM PV unit's maximum power is determined by available solar irradiance and varies with environmental conditions; it adjusts system frequency

TABLE I: Summary of test cases

| | MGMS Functions | System Conditions | Testing Duration |
|---|---|---|---|
| #0: Baseline scenario | Generation and load balance | No BESS, PV operates in MPPT, and the gas generator is on, high load and low PV | 24 hours |
| #1: Islanded energy management | 1) Coordinate the near-term power generation and consumption during island operation. 2) Meet the island survival performance expectations while maximizing customer reliability. | High load and low PV | 24 hours |
| #2: Islanded secondary control | Regulate the system frequency to nominal during the dynamic change of load and solar production. | High load and low PV | 30 minutes |
| #3: Island constraint management | Coordinate the microgrid assets (DERs, capacitor banks) to relieve constraints on the feeder during islanded operation. | An over voltage scenario is created with high PV and low load. | 30 minutes |
| #4: Autonomous islanding operation | The microgrid system should go to unplanned islanding and survive. If not, the MGMS should launch a black start. | An upstream fault will be simulated so that the microgrid POI relay opens the breaker. High load and low PV. | 5 minutes |
| #5: Autonomous synchronization operation | The microgrid will send control signals to the POI relay to synchronize to the grid, and the MGMS should also send the signal to the GFM inverters to adjust their output voltages to make the microgrid-side voltages close to the grid-side voltages. | The main grid is back to normal, and the MGMS receives the signal from the user to reconnect to the grid. High load and low PV. | 5 minutes |

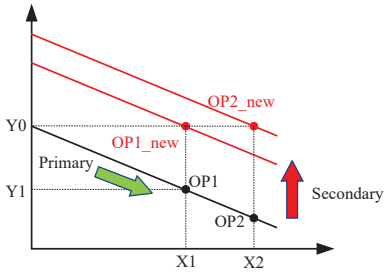


Fig. 9: MGMS secondary controls.

with a vertical $P$-$f$ droop curve when operating power reaches maximum or minimum levels. The gas generator requires a positive minimum power output, and the MGMS coordinates with other DERs to maintain the generator's output above this threshold. This comprehensive droop setting configuration ensures effective load sharing and frequency regulation among the GFM units and the gas generator, maintaining system stability and efficiency.

### C. Test Cases

The experimental tests are performed based on the test scenarios defined in Table I. Note that all test scenarios focus on the islanded operation to evaluate the microgrid controller's ability to improve the microgrid reliability and resiliency when the wider-area grid is unavailable.

## IV. Test Case Results and Validations

This section demonstrates the CHIL-based simulation from the laboratory setups. Due to the page limit, this paper only showcases part of the test results.

### A. Test Case #0

In this test case, the system operates in island mode with feeder head breakers T1 and T2 open and tie-breaker T3 closed, isolating the system. The 4.8 MVA diesel generator is the primary power source, supplying only critical loads (Load B, G, H, and I), while most capacitors are disconnected except for CAP1. All BESS units are also disconnected, and the GFM PV unit is replaced with a legacy unit (PV 3 in Figure 1).

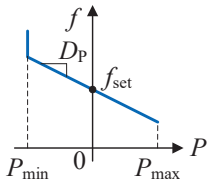


(a) $P$-$f$ droop ($D_P$=1.6%).

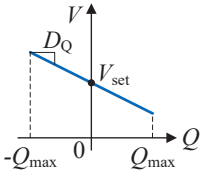


(b) $Q$-$V$ droop ($D_Q$=1%).

Fig. 10: Droop settings for GFM BESS unit.

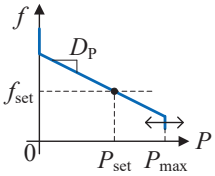


(a) $P$-$f$ droop ($D_P$=1.6%).

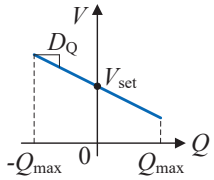


(b) $Q$-$V$ droop ($D_Q$=1%).

Fig. 11: Droop settings for GFM PV unit.

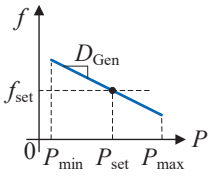


(a) $P$-$f$ droop ($D_{Gen}$=5%).

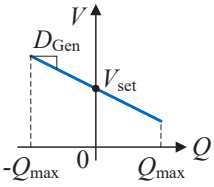


(b) $Q$-$V$ droop ($D_{Gen}$=5%).

Fig. 12: Droop settings for gas generator.

The CHIL-based simulation for the baseline case, characterized by high PV generation, begins at 7 a.m. and runs for 24 hours. This timing ensures a meaningful comparison with Test Case #1 by capturing the morning increase in solar irradiance, essential for the renewable energy devices in Test Case #1. Measurements taken include frequency and voltages at the point of interconnection (T1) and the active/reactive power from the diesel generator. The MGMS controller dispatches active/reactive power set points to the generator.

Simulation results show that the MGMS controller can adjust the generator's $P$-$f$ and $Q$-$V$ droop settings to maintain system frequency and voltage around 60 Hz and 1 p.u. The results also illustrate that PV units cease power generation

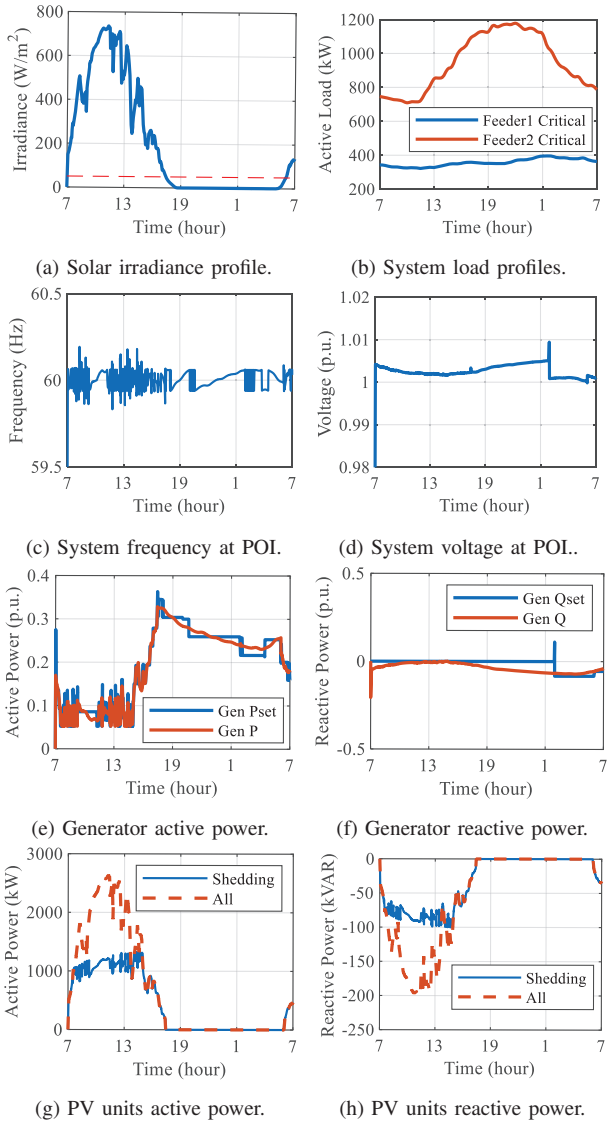


(a) Solar irradiance profile. (b) System load profiles.

(c) System frequency at POI. (d) System voltage at POI..

(e) Generator active power. (f) Generator reactive power.

(g) PV units active power. (h) PV units reactive power.

Fig. 13: Results for the Test Case #0 of a summer case.

when solar irradiance drops below 50 W/m$^2$. The critical loads are modeled as constant impedance loads with a leading power factor of 0.9. The figures demonstrate the power generation capabilities of the diesel generator and the PV units, highlighting the MGMS controller's effectiveness in maintaining stable operation in an islanded mode.

### *B. Test Case #1*

In this test case, the MGMS controller manages power generation and consumption across two microgrid systems during islanded operations, starting from a black-start scenario, and dispatching GFM and GFL units without the diesel generator. The black-start procedure begins with BESS3, the largest-capacity unit, followed by the sequential closing of circuit breakers to bring loads online and enable the synchronization of BESS2 to BESS3. Once all loads are reconnected, the GFM PV and GFL units are brought online, with all BESS starting at 80% state of charge (SOC).

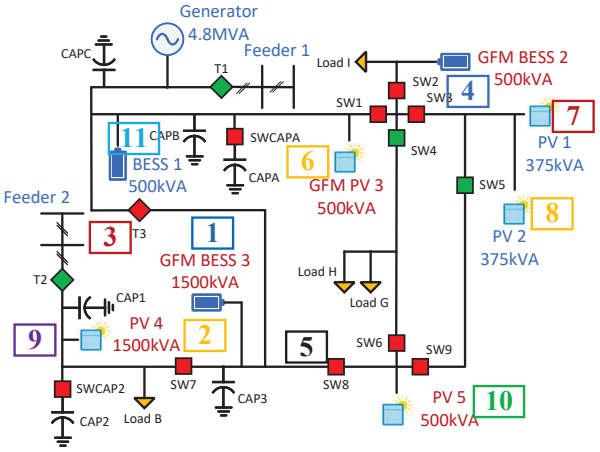


Fig. 14: System black-start sequence.

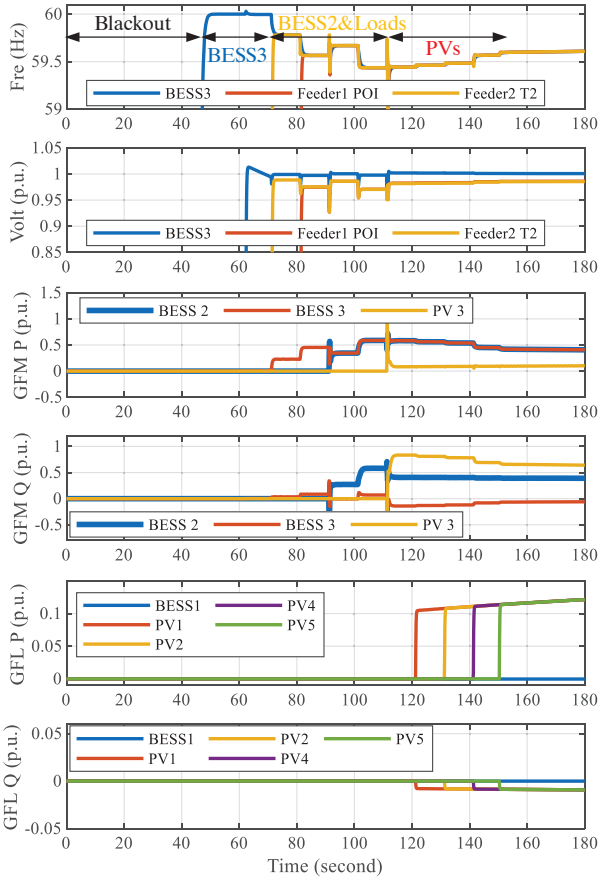


Fig. 15: System black-start results.

The results in Figure 15 indicate that BESS3 connects at 63 seconds, and sequential circuit breaker closures restore various loads. The GFM PV unit operates in active power reserve mode, while GFL PV units maximize energy output in MPPT mode, with GFL BESS units set to zero power dispatch as backup. During the summer scenario, PV1 and PV2 are intentionally shut down between 11 a.m. and 2 p.m. due to BESS1 and BESS3 reaching 95% SOC. Normal operation resumes when SOC drops below 95%. The system functions until BESS1's SOC reaches 20% at 17.7 hours, transitioning

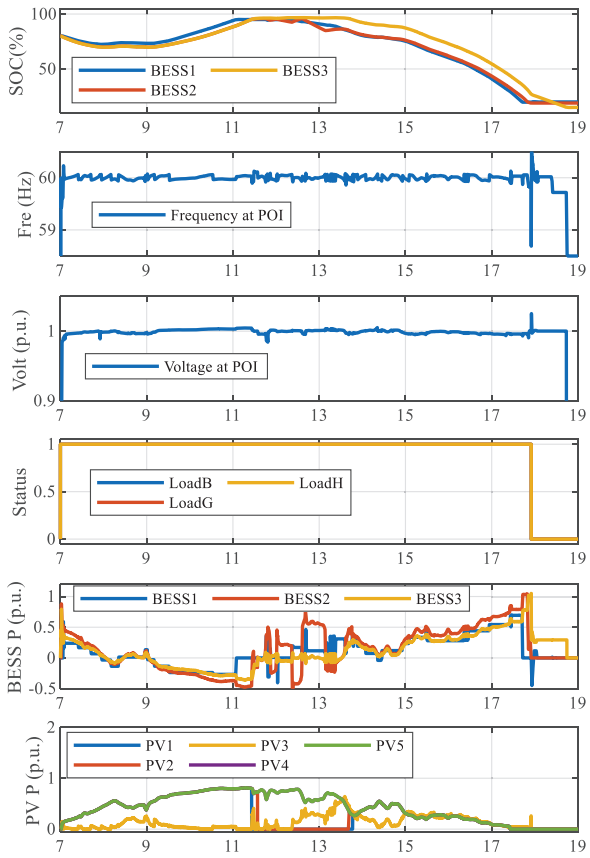


Fig. 16: Results for the Test Case #1 of a summer case.

it to standby mode, and BESS2 disconnects at 19% SOC.

After BESS2 disconnects, system frequency drops below 58.7 Hz, triggering load-tripping procedures and disconnecting loads B, G, and H. BESS3 continues to supply Load I until its SOC drops below 20%, transitioning to standby mode and disconnecting at 15% SOC. With no PV generation at 18.7 hours, system voltage falls below 0.9 p.u., leading to the tripping of all remaining units and a total operation time of about 11.7 hours. This sequence highlights the system's stability and reliability under varying conditions.

### C. Test Case #2

In this test case, the MGMS controller manages island operations autonomously by regulating system frequency and maintaining POI voltage using GFM inverters while the microgrid remains isolated from the main grid. The setup includes open feeder head breakers T1 and T2 and a closed tie-breaker T3, with only GFM and GFL units involved. The simulation focuses on a low-load, high-PV summer scenario, assessing the MGMS controller's ability to maintain stability under such conditions. Results in Figure 17 show that the MGMS effectively maintains frequency and voltage stability, with BESS2 and BESS3 being charged by PV units due to adjusted frequency set points. It also highlights the system's frequency, voltage, and command set points, demonstrating how GFM inverters adapt their control set points to shift the droop settings and maintain operational stability.

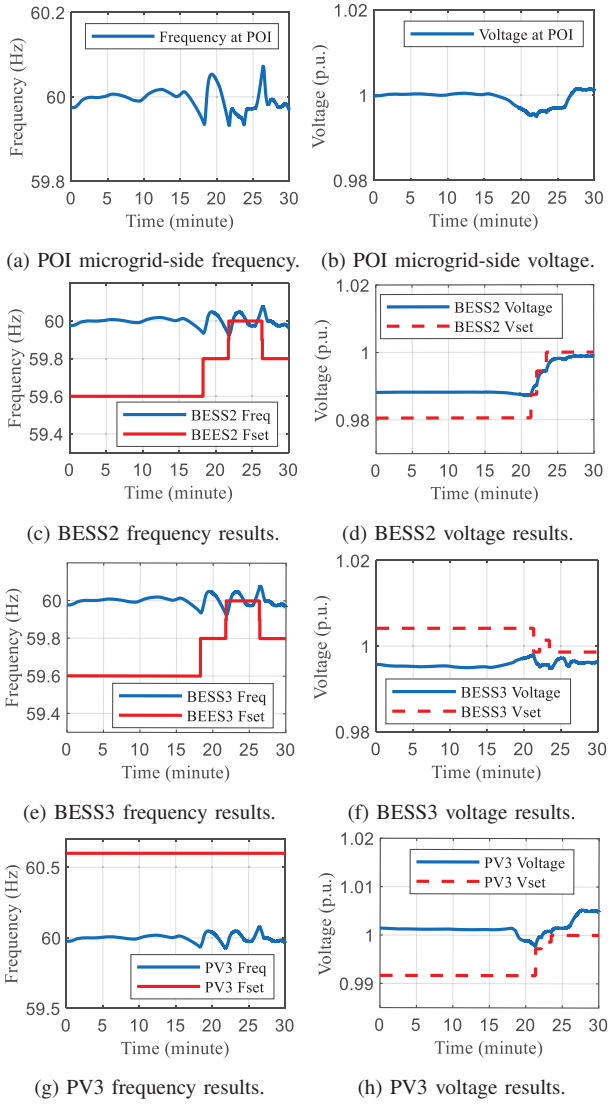


(a) POI microgrid-side frequency. (b) POI microgrid-side voltage.

(c) BESS2 frequency results. (d) BESS2 voltage results.

(e) BESS3 frequency results. (f) BESS3 voltage results.

(g) PV3 frequency results. (h) PV3 voltage results.

Fig. 17: Results for the Test Case #2 of a summer case.

### D. Test Case #5

In this scenario, the MGMS initiates the microgrid's reconnection to the main grid by issuing a reconnection signal. The GFM units adjust their output voltage and frequency to align with the main grid, ensuring smooth and stable synchronization. The POI circuit breaker T1 closes once the voltage, frequency, and phase angle differences between the microgrid and the main grid fall within acceptable thresholds: 30 V for voltage magnitude, 0.05 Hz for frequency, and 0.05 radians for phase angle difference.

The simulation settings are consistent with those in Test Case #2, ensuring uniformity and comparability. After reconnection, the frequency and voltage stabilize around their nominal values, so the MGMS will not issue new command set points to the GFM units, as their output will already align with the main grid's requirements. This approach ensures seamless integration and stable operation of the microgrid within the larger power system, consistent with the UNIFI 1 MW demo smooth transition protocol.

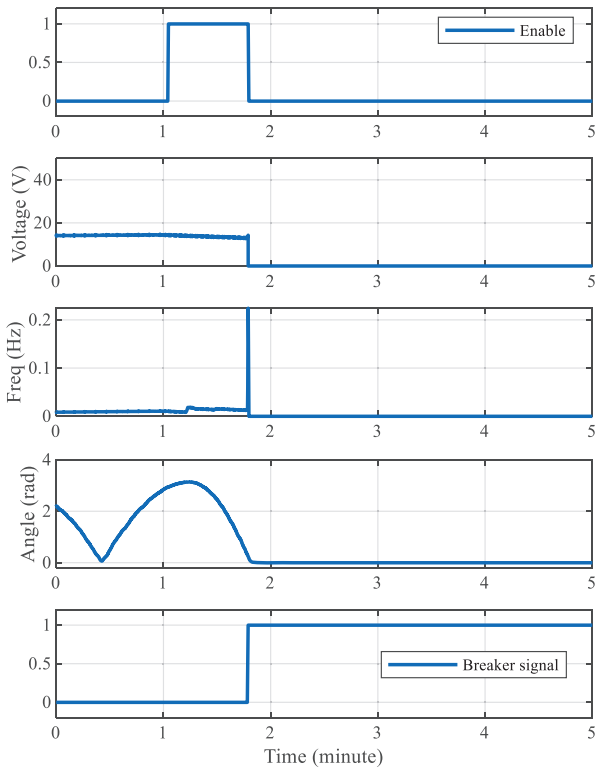


Fig. 18: Measurement of POI breaker T1.

Figures provide detailed measurements and results of the resynchronization process, showing the measurements from the POI breaker T1 and the system- and device-specific frequency and voltage adjustments during resynchronization. The frequency control interval is refined to 0.01 Hz to ensure precise synchronization. The figures display the active and reactive power outputs from the GFM units, highlighting their contributions to maintaining power balance and system stability throughout the resynchronization. These results collectively demonstrate the system's ability to maintain stable frequency, voltage, and power distribution across all connected units during and after the resynchronization process.

### *E. Summary of Test Cases*

In the Baseline Case, we conducted 24 hours simulation for both summer and winter cases starting from 7 a.m. As shown in Figure 13, the maximum active load is approximately 1.6 MW while the diesel generator-rated active power is 4.8 MW. Therefore, the diesel generator can supply all critical loads for 24 hours without shedding any loads. However, due to the limit of minimum generator power, PV units are turned off during the noon time of the summer case. The total critical load energy is obtained by integrating load profiles in Figure 13(b):

$$E_{crld} = \int_0^{24h} \text{profiles } dt = 31406\text{kWh} \tag{1}$$

The total generation energy from the generator and all PV units can be calculated as:

$$E_{Gen} = \int_0^{24h} P_{Gen}\ dt = 22351\text{kWh} \tag{2}$$

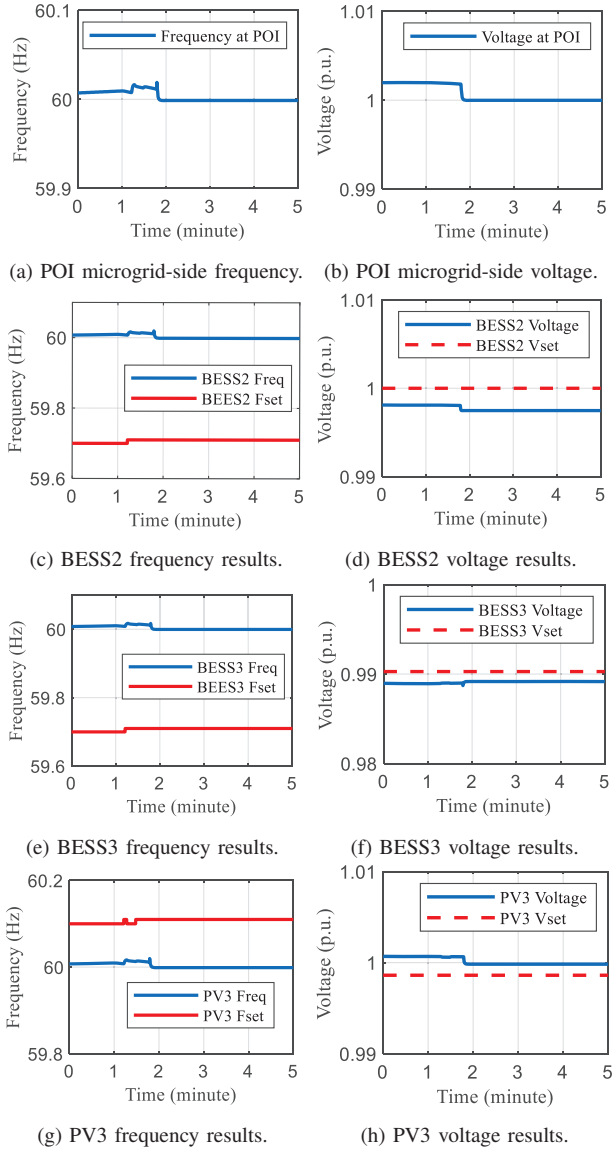


(a) POI microgrid-side frequency. (b) POI microgrid-side voltage.

(c) BESS2 frequency results. (d) BESS2 voltage results.

(e) BESS3 frequency results. (f) BESS3 voltage results.

(g) PV3 frequency results. (h) PV3 voltage results.

Fig. 19: Results for the Test Case #5 of a summer case.

$$E_{PV} = \sum_{n=1}^{5} \int_0^{24h} P_{PV,n}\ dt = 10448\text{kWh} \tag{3}$$

In Test Case #1, simulations of an islanded microgrid system were conducted for a summer scenario starting from a complete blackout, successfully energizing all devices. The system, with a maximum active load of approximately 1.6 MW, relied on BESS units to supply critical loads. However, varying PV generation and the SOC in the BESS units necessitated the shutdown of certain PV devices to prevent overcharging. The entire system was shut down when insufficient power was available to protect the microgrid components. The system was energized at 7 a.m. with an 80% SOC for all BESS units and was completely shut down by 6:44 p.m., resulting in a survival time of approximately 11.74 hours. Loads B, G, and H were shut down around 5:44 p.m., after 10.91 hours, due to a frequency drop. The total required critical load energy $E_{crld}^{req}$

is obtained by integrating load profiles in Figure 13(b):

$$E_{crld}^{req} = \int_0^{11.74h} \text{profiles } dt = 14094\text{kWh} \quad (4)$$

The total served energy for critical load $E_{crld}^{srvd}$ is:

$$E_{crld}^{srvd} = \sum_{n=B,G,H} \int_0^{10.91h} P_{Load,n}\ dt + \int_0^{11.74h} P_{LoadI}\ dt = 13203\text{kWh} \quad (5)$$

A metric, the "percentage of critical load served," is thus defined to evaluate how MGMS is able to serve the total critical load during islanding operations. It is obtained as:

$$Srvd_{crld} = \frac{E_{crld}^{srvd}}{E_{crld}^{req}} * 100\% = 93.68\% \quad (6)$$

The metric "critical load interruption time" is design to evaluate MGMS ability to maintain supply continuity during islanded operations for individual critical loads. The metrics for Loads B, G, and H are defined as:

$$Intrpt_{crld} = \frac{T_{crld}^{shed}}{T_{island}} * 100\% = 7.07\% \quad (7)$$

where $T_{crld}^{shed}$ is the critical load shedding duration and $T_{island}$ is the islanding duration. The total generation energy from the BESS units and PV units can be calculated as:

$$E_{BESS} = \sum_{n=1}^{3} \int_0^{11.74h} P_{BESS,n}\ dt = 3220\text{kWh} \quad (8)$$

$$E_{PV} = \sum_{n=1}^{5} \int_0^{11.74h} P_{PV,n}\ dt = 13269\text{kWh} \quad (9)$$

The goal of Test Case #2 is to evaluate the MGMS's capability to provide secondary frequency and voltage control during island operation, aiming to restore steady-state voltage and frequency deviations. The effectiveness of this control is measured using the metrics average frequency deviation, $fD_{\%}$, which evaluates the average frequency violation, and maximum frequency deviation, $fD_{max}$, which assesses the controller's behavior during system disturbances.

$$fD_{\%} = \frac{\sqrt{\sum_t (f_t - f_{set})^2}}{T^2 * f_{set}} * 100\% = 0.05\% \quad (10)$$

$$fD_{max} = \max_t \left(\frac{|f_t - f_{set}|}{f_{set}}\right) * 100\% = 0.18\% \quad (11)$$

where $f_t$ is the frequency measurements over the time windows $T$, and $f_{set}$ is the frequency set point (60 Hz).

Similar metrics are defined for voltage control of each phase to calculate the average voltage deviation and the average voltage deviation. The evaluation metrics for Phase $B$ are:

$$VD_{\%PhB} = \frac{\sqrt{\sum_t (V_t - V_{set})^2}}{T^2 * V_{set}} * 100\% = 0.85\% \quad (12)$$

$$fD_{maxPhB} = \max_t \left(\frac{|V_t - V_{set}|}{V_{set}}\right) * 100\% = 1.41\% \quad (13)$$

In Test Case #5, the microgrid begins in a stable islanded operational state. When the main grid is available, The MGMS controller dispatches DERs to resynchronize to the upstream system and create a closed transition from islanded to grid-connected operation without causing disruptions. At the end of the test case, the microgrid reconnects to the main grid.

For Test Case #3, an overvoltage condition caused by high PV generation and low load demand is simulated and the MGMS coordinates GFM DERs during island operations to manage system voltage and frequency. In Test Case #4, an upstream fault is detected by the microgrid POI relay T1, which opens the circuit breaker to transition the microgrid to islanded mode. Simulation results demonstrate that the microgrid maintains stability and continues to operate effectively.

## V. Conclusion

This paper presents the CHIL-based evaluation of the MGMS controller, demonstrating the system's robustness and adaptability in managing a microgrid with multiple GFM inverters and high renewable energy penetration. By simulating various operational scenarios, these case studies highlight the MGMS's capability to maintain system stability, balance power generation, and consumption, and ensure continuous supply to critical loads. The results indicate that the MGMS effectively dispatches GFM inverters of BESS units and PV units, manages operational constraints, and provides secondary frequency and voltage control. This evaluation demonstrates the potential of advanced MGMS to enhance the resilience and reliability of microgrids, facilitate greater integration of DERs into power systems, and utilize GFM resources to provide and maintain system frequency.

## References


[1] J. Wang, C. Zhao, A. Pratt, and M. Baggu, "Design of an Advanced Energy Management System for Microgrid Control Using a State Machine," Elsevier, Applied Energy, vol. 228, pp. 2407-2421.

[2] J. Wang, S. Ganguly, and B. Kroposki, "Study of Seamless Transition Operation Using Grid-Forming Inverters," IECON 2023—49th Annual Conference of the IEEE Industrial Electronics Society.

[3] M. F. Zia, E. Elbouchikhi, M. Benbouzid, "Microgrid Energy Management Systems: A Critical Review on Methods, Solutions, and Prospects," Applied Energy, vol. 222, July 2018, pp. 1033-1055.

[4] R. G. Allwyn, A. Al-Hinai, V. Margaret, "A Comprehensive Review on Energy Management Strategy of Microgrids," Energy Reports 9 (2023), pp. 5565-5591.

[5] J. Comden and J. Wang, "An Innovative Energy Management System for Microgrids with Multiple Grid-Forming Inverters," 2024 IEEE Power & Energy Society General Meeting (PESGM).

[6] Quan, Xiangjun, et al. "Photovoltaic synchronous generator: Architecture and control strategy for a grid-forming PV energy system." IEEE Journal of Emerging and Selected Topics in Power Electronics 8.2 (2019): 936-948.

[7] Shah, Chinmay, et al., "High-Fidelity Model of Stand-Alone Diesel Electric Generator With Hybrid Turbine-Governor Configuration for Microgrid Studies." IEEE Access 10 (2022): 110537-110547.

[8] Siemens Microgrid Management Systems. Available: https://xcelerator.siemens.com/global/en/all-offerings/services/m/microgrid-mgms-based-services.html

[9] Controller Requirements for Managing Community Microgrids: Reference Requirements Language for Implementation of Microgrid Controls. EPRI, Palo Alto, CA: 2022. 3002025648.

[10] 2030.7-2017-IEEE Standard for the Specification of Microgrid Controller. Available:https://ieeexplore.ieee.org/document/8340204.